Memorias del 2024 Congreso Nacional de Control Automático
8-11 de Octubre, 2024. Ciudad de México, México.

Consensus Control of Nonholonomic Vehicles with Input Constraints and Time-Varying Delays ⋆

Angel I. Paredes * **Emmanuel Nuño** * **Antonio Loría** **

* *Department of Computer Sciences, CUCEI, University of Guadalajara, Jalisco, Mexico (e-mail: angel.paredes@alumnos.udg.mx; emmanuel.nuno@academicos.udg.mx).*
** *L2S-CentraleSupelec, CNRS, 3 Rue Joliot Curie, Gif-sur-Yvette, France (e-mail: antonio.loria@cnrs.fr).*

Abstract: This paper proposes a solution to the consensus formation control problem for agents with nonholonomic constraints and network communications subject to time-varying delays. The proposed controller addresses the consensus paradigm using a bounded input design without requiring velocity measurements. Network communications between the agents occur over an undirected graph topology. In order to deal with the nonholonomic constraints we design the controller to be time-varying using a persistence of excitation term. A comparative simulation analysis, with an unbounded control scheme, is provided.

Keywords: Multi-agent systems, formation control, consensus control, nonholonomic systems, time-varying delays.

1. INTRODUCTION

Formation consensus is a widely studied problem in multi-agent systems due to its significant potential. Nonholonomic restrictions are a common characteristic among mobile vehicle configurations, leading to a plethora of works aimed at solving the formation consensus control problem (Dimarogonas and Kyriakopoulos, 2007; Lin et al., 2005; Ajorlou et al., 2015; Peng et al., 2015; Cheng et al., 2018). Most of these works assume ideal communication channels with no delays, require velocity measurements to be available, or are prone to saturating the agents actuators. In reality, the communications are affected by time delays, and thus, controllers for multi-agent systems must be robust to this phenomenon (Cao and Ren, 2011; Wang, 2014; Hatanaka et al., 2015). Similarly, velocity measurements are not always available, as the fidelity of these signals can be compromised due to the lack of dedicated sensors or their defects. In view of this, designing controllers that rely solely on position and orientation measurements is a recommended strategy (Liang et al., 2018). Finally, assuming ideal actuators without considering saturation can lead to system underperformance, mechanical or thermal failure of the actuators, and compromise task achievement. Therefore, proper controller design that avoids actuator saturation is always advisable (Loría et al., 1997; Zavala-Río et al., 2011).

The work of Paredes-Lopez et al. (2022) addresses a consensus problem considering actuator saturation, without requiring measurable velocities, and accounts for time delays in communications. However, this approach does not apply to nonholonomic vehicles. In the recent paper (Romero et al., 2024), an output-feedback controller for the consensus-based formation problem of nonholonomic vehicles with delayed communications is reported. Nonetheless, these works assume the unrealistic condition that the actuators are ideal and thus that do not saturate.

The controller design in the present work aims at solving the open problem of bounded input consensus-based formation control for nonholonomic agents with time-varying communication delays and without velocity measurements. To achieve this, a smooth decentralized controller is implemented, where the lack of velocity measurements is compensated by a virtual dynamic controller. This virtual controller is interconnected with the agents and effectively injects damping using a passivity-based approach. It also accounts for the network interconnection between the agents virtual dynamics, enabling us to reach the consensus formation objective and establish proper stability conditions to handle time-varying bounded delays with also bounded derivatives. Finally, the nonholonomic constraints are addressed by implementing a persistence of excitation term, similar to our previous schemes (Nuño et al., 2022; Loría et al., 2022). This term is added

⋆ This work has been supported by the Mexican CONAHCYT Research Grant CBF-2023-2024-1964. The first author acknowledges CONAHCYT for his scholarship with CVU 1088222.

https://doi.org/10.58571/CNCA.AMCA.2024.059

to the virtual controller dynamics and only vanishes when the desired control objective is successfully achieved.

2. PROBLEM SETTING

This work addresses a formation control problem for a group of N differential-drive vehicles with nonholonomic constraints using a consensus algorithm. These vehicles move in a three-dimensional space $\mathbf{x}_i = [x_i, y_i, \theta_i]^\top \in \mathbb{R}^3$. Each vehicle's kinematics are described by:

$$\dot{\mathbf{x}}_i = \mathbf{G}(\mathbf{x}_i)\mathbf{v}_i := \begin{bmatrix} \cos(\theta_i) & 0 \\ \sin(\theta_i) & 0 \\ 0 & 1 \end{bmatrix} \mathbf{v}_i, \tag{1}$$

where $\mathbf{v}_i := [v_i, \omega_i]^\top \in \mathbb{R}^2$ represents linear and angular velocities respectively. The vehicle dynamics are expressed as

$$\mathbf{M}_i\dot{\mathbf{v}}_i + \mathbf{F}_i\mathbf{v}_i = \mathbf{B}_i\boldsymbol{\tau}_i, \tag{2}$$

where $\mathbf{M}_i, \mathbf{F}_i, \mathbf{B}_i$, are the mass, the friction and the input matrices, respectively.

Our control design uses an inner control-loop given by:

$$\boldsymbol{\tau}_i = \mathbf{B}_i^{-1}\mathbf{u}_i,$$

where $\mathbf{u}_i := [u_{vi}, u_{\omega i}]^\top$ is the consensus-based controller. For differential wheel drive vehicles, $\mathbf{B}_i$ is

$$\mathbf{B}_i = \frac{1}{r_i}\begin{bmatrix} 1 & 1 \\ 2R_i & -2R_i, \end{bmatrix}$$

where r_i is the wheel radius, and R_i is the wheel axle length. This leads to the following dynamics for linear and angular velocities:

$$\boldsymbol{\tau}_i = \frac{r_i}{2}\begin{bmatrix} 1 & \frac{1}{2R_i} \\ 1 & -\frac{1}{2R_i} \end{bmatrix}\begin{bmatrix} u_{vi} \\ u_{\omega i} \end{bmatrix}. \tag{3}$$

This last and the fact that $\mathbf{M}_i := \mathrm{diag}(m_i, I_i)$ and $\mathbf{F}_i := \mathrm{diag}(f_{vi}, f_{\omega i})$ yields the following second order linear and angular velocities dynamics

$$\dot{v}_i = \frac{1}{m_i}\left(u_{vi} - f_{vi}v_i\right) \tag{4a}$$

$$\dot{\omega}_i = \frac{1}{I_i}\left(u_{\omega i} - f_{\omega i}\omega_i\right) \tag{4b}$$

where I_i is the robot inertia, m_i is the mass, f_{vi}, $f_{\omega i}$ are the friction coefficients.

In this scenario, we assume that only pose of the vehicles are available for measurement and input torques are prone to saturation. Thus the following assumptions.

Assumption 1. The Cartesian position (x_i, y_i) and the orientation θ_i, for each vehicle, are available. ◁

Assumption 2. The wheel torques $\boldsymbol{\tau}_i := [\tau_{li}, \tau_{ri}]^\top$ can be saturated and thus they satisfy $|\tau_{li}| \leq \bar{\tau}_{li}$ and $|\tau_{ri}| \leq \bar{\tau}_{ri}$ for the left and right wheel respectively, where $\bar{\tau}_{li} > 0$ and $\bar{\tau}_{li} > 0$ are assumed *known.* ◁

Let $\boldsymbol{\delta}_i \in \mathbb{R}^2$ be a constant vector determining the position of the ith vehicle relatively to the formation center and, correspondingly, let $\bar{\mathbf{z}}_i := \mathbf{z}_i - \boldsymbol{\delta}_i$ denote its relative position error, where $\mathbf{z}_i := [x_i, y_i]^\top$. The control goal is for the vehicles to reach a desired formation around an unspecified rendezvous point. $\mathbf{z}_c := (x_c, y_c)$, with a common orientation θ_c. Thus, we aim to ensure:

$$\lim_{t\to\infty} v_i(t) = 0, \quad \lim_{t\to\infty} \bar{\mathbf{z}}_i(t) = \mathbf{z}_c, \tag{5}$$

$$\lim_{t\to\infty} \omega_i(t) = 0, \quad \lim_{t\to\infty} \theta_i(t) = \theta_c \qquad \forall\, i \in N. \tag{6}$$

Then, for further development, we rewrite the kinematics model (1) as

$$\dot{\bar{\mathbf{z}}}_i = \boldsymbol{\varphi}(\theta_i)v_i; \qquad \boldsymbol{\varphi}(\theta_i) := [\cos(\theta_i) \quad \sin(\theta_i)]^\top \tag{7}$$

$$\dot{\theta}_i = \omega_i. \tag{8}$$

Vehicles exchange information with their neighbors $\mathcal{N}_i$. Communication between two vehicles i and $j \in \mathcal{N}_i$ is bidirectional and never lost. Hence the following.

Assumption 3. The interconnections are static and are modeled via an undirected and connected graph. ◁

We model the interconnection graph with a constant Laplacian matrix, $\mathbf{L} := [\ell_{ij}] \in \mathbb{R}^{N\times N}$, where

$$\ell_{ij} = \begin{cases} \sum_{k\in\mathcal{N}_i} a_{ik} & i = j \\ -a_{ik} & i \neq j, \end{cases} \tag{9}$$

By construction, $\mathbf{L}\mathbf{1}_N = 0$, where $\mathbf{1}_N = [1\cdots 1]^\top$ and, after Assumption 3, $\mathbf{L}$ is symmetric, it has a unique zero-eigenvalue, and the rest of its spectrum is strictly positive. Thus, $\mathrm{rank}(\mathbf{L}) = N - 1$.

Furthermore, communication from the jth to the ith vehicle is subject to a variable time-delay, $T_{ji}(t)$ with the following characteristics:

Assumption 4. $T_{ji}(t)$ is bounded by a known upper-bound $\overline{T}_{ji} \geq 0$ and has bounded time-derivatives. ◁

3. PROPOSED CONTROL SCHEME

The agents motion dynamics can be split into angular and linear components. The output-feedback controller design is divided similarly, with separate controllers each motion dynamics.

3.1 Angular control

Consider the controlled second-order dynamical system

$$\ddot{\vartheta}_{\omega i} + d_{\omega i}\dot{\vartheta}_{\omega i} + p_{\omega i}\tilde{e}_{\omega i} = \nu_{\omega_i} \tag{10}$$

where $\dot{\vartheta}_{\omega i}, \vartheta_{\omega i} \in \mathbb{R}$ are the controllers angular velocity and orientation, respectively, $\tilde{e}_{\omega i}$ is the interconnection error between the neighbors virtual dynamics defined as

$$\tilde{e}_{\omega i} := \sum_{j\in\mathcal{N}_i} a_{ij}\left[\vartheta_{\omega i} - \vartheta_{\omega j}(t - T_{ji}(t))\right] \tag{11}$$

ν_{ω_i} is an external input and $p_{\omega i}, d_{\omega i} > 0$ are the proportional and the damping injection gains, respectively.

https://doi.org/10.58571/CNCA.AMCA.2024.059

Define the input $\nu_{\omega i} := k_{\omega i}\tanh(\theta_i - \vartheta_{\omega i}) + \alpha_i$, hence

$$\begin{aligned}\ddot{\vartheta}_{\omega i} =& - d_{\omega i}\dot{\vartheta}_{\omega i} - p_{\omega i}\tilde{e}_{\omega i} + k_{\omega i}\tanh(\theta_i - \vartheta_{\omega i})\\ &+ \alpha_i(t, \theta_i, \boldsymbol{\vartheta}_{vi}, \bar{\mathbf{z}}).\end{aligned} \tag{12}$$

Set the controller $u_{\omega i}$ as

$$u_{\omega i} = -k_{\omega i}\tanh(\theta_i - \vartheta_{\omega i}), \quad k_{\omega i} > 0, \tag{13}$$

then, the closed-loop system corresponding to the angular-motion dynamics results in

$$\Sigma_{vi} := \begin{cases} \dot{\theta}_i = \omega_i \\ \dot{\omega}_i = -\dfrac{1}{I_i}\left[k_{\omega i}\tanh(\theta_i - \vartheta_{\omega i}) + f_{\omega i}\omega_i\right] \\ \ddot{\vartheta}_{\omega i} = - d_{\omega i}\dot{\vartheta}_{\omega i} - p_{\omega i}\tilde{e}_{\omega i} + k_{\omega i}\tanh(\theta_i - \vartheta_{\omega i}) \\ \qquad + \alpha_i(t, \theta_i, \boldsymbol{\vartheta}_{vi}, \bar{\mathbf{z}}). \end{cases} \tag{14}$$

Here, α_i, is defined as follows

$$\alpha_i(t, \theta_i, \boldsymbol{\vartheta}_{vi}, \bar{\mathbf{z}}) := k_{\alpha i}\psi_i(t)\boldsymbol{\varphi}(\theta_i)^{\perp\top}\mathbf{tanh}(\boldsymbol{\vartheta}_{vi} - \bar{\mathbf{z}}_i), \tag{15}$$

where constant $k_{\alpha i} > 0$ and $\boldsymbol{\varphi}(\theta_i)^{\perp} := [-\sin(\theta_i)\ \cos(\theta_i)]^\top$, is the annihilator of $\boldsymbol{\varphi}(\theta_i)$, satisfying $\boldsymbol{\varphi}(\theta_i)^{\perp\top}\boldsymbol{\varphi}(\theta_i) = 0$.

Assumption 5. For each $i \leq N$, ψ_i in (15) is bounded and differentiable. There exists $\bar{\psi}_i > 0$ such that

$$\max\{\sup_{t\geq 0}|\psi_i(t)|, \ \sup_{t\geq 0}|\dot{\psi}_i(t)|\} \leq \bar{\psi}_i,$$

as well as μ_i and $T_i > 0$ such that

$$\int_t^{t+T}\dot{\psi}_i(s)^2 ds \geq \mu, \qquad \forall\, t \geq 0. \tag{16}$$

The function α_i is designed to be a uniformly δ-PE function with respect to $h(\theta_i, \bar{\mathbf{z}}_i, \boldsymbol{\vartheta}_{vi}) := \boldsymbol{\varphi}(\theta_i)^{\perp\top}\mathbf{tanh}(\boldsymbol{\vartheta}_{vi} - \bar{\mathbf{z}}_i)$—cf. (Loría et al., 2005). In other words, α_i remains persistently exciting as long as $\boldsymbol{\varphi}(\theta_i)^{\perp\top}\mathbf{tanh}(\boldsymbol{\vartheta}_{vi}-\bar{\mathbf{z}}_i) \neq 0$

3.2 Linear control

As for the linear-motion dynamics, the controllers are given by the set of equations

$$u_{vi} = -k_{vi}\boldsymbol{\varphi}(\theta_i)^\top\mathbf{tanh}(\bar{\mathbf{z}}_i - \boldsymbol{\vartheta}_{vi}) \tag{17}$$

$$\ddot{\boldsymbol{\vartheta}}_{vi} = -d_{vi}\dot{\boldsymbol{\vartheta}}_{vi} - p_{vi}\tilde{\mathbf{e}}_{vi} + k_{vi}\boldsymbol{\varphi}(\theta_i)^\top\mathbf{tanh}(\bar{\mathbf{z}}_i - \boldsymbol{\vartheta}_{vi}), \tag{18}$$

where $\mathbf{tanh}(\boldsymbol{\vartheta}_{vi}-\bar{\mathbf{z}}_i) := [\tanh(\vartheta_{xi} - \bar{x}_i)\ \tanh(\vartheta_{yi} - \bar{y}_i)]^\top$ and

$$\tilde{\mathbf{e}}_{vi} := \sum_{j\in\mathcal{N}_i} a_{ij}\Big[\boldsymbol{\vartheta}_{vi} - \boldsymbol{\vartheta}_{vj}(t - T_{ji}(t))\Big]. \tag{19}$$

In closed loop with (4a)-(7), we obtain the closed-loop system's equations

$$\Sigma_{vi} := \begin{cases} \dot{\bar{\mathbf{z}}}_i = \boldsymbol{\varphi}(\theta_i)v_i \\ \dot{v}_i = -\dfrac{1}{m_i}\left[f_{vi}v_i + k_{vi}\boldsymbol{\varphi}(\theta_i)^\top\mathbf{tanh}(\bar{\mathbf{z}}_i - \boldsymbol{\vartheta}_{vi})\right] \\ \ddot{\boldsymbol{\vartheta}}_{vi} = - d_{vi}\dot{\boldsymbol{\vartheta}}_{vi} - k_{vi}\mathbf{tanh}(\boldsymbol{\vartheta}_{vi} - \bar{\mathbf{z}}_i) - p_{vi}\tilde{\mathbf{e}}_{vi}. \end{cases} \tag{20}$$

Proposition 1. Consider the system (2) in closed loop with the controller defined by (13), (12), (17), and (18). Then, the following hold.

(i) Let k_{vi} and $k_{\omega i}$, be positive constants such that, for any given saturation levels $\bar{\tau}_{li}$ and $\bar{\tau}_{ri}$

$$\frac{4R_i}{r_i}\min\{\bar{\tau}_{li},\ \bar{\tau}_{ri}\} > 2\sqrt{2}R_ik_{vi} + k_{\omega i}. \tag{21}$$

Then, the left and right torques satisfy $|\tau_{li}| < \bar{\tau}_{li}$ and $|\tau_{ri}| < \bar{\tau}_{ri}$, so the actuators do not saturate.

(ii) If Assumptions 2–3 hold and, for any $i \leq N$,

$$d_{vi} > \frac{1}{2}p_{vi}\sum_{i\in\mathcal{N}_i}a_{ij}\left(\beta_i + \frac{\bar{T}_{ji}^2}{\beta_j}\right), \tag{22}$$

$$d_{\omega i} > \frac{1}{2}p_{\omega i}\sum_{i\in\mathcal{N}_i}a_{ij}\left(\varepsilon_i + \frac{\bar{T}_{ji}^2}{\varepsilon_j}\right), \tag{23}$$

for all $j \in \mathcal{N}_i$, $\varepsilon_i > 0$, and $\beta_i > 0$ arbitrarily chosen, the desired control objectives (5) and (6) hold for any initial conditions.

4. PROOF OF THE MAIN RESULT

Consider the linear-motion closed-loop dynamics Σ_{vi} in (20) and the Lyapunov-Krasovskii functional

$$V := \sum_{i=1}^N\left[\frac{1}{p_{vi}}\mathcal{E}_{vi} + \Upsilon_{vi} + \frac{1}{4}\sum_{j\in\mathcal{N}_i}a_{ij}|\boldsymbol{\vartheta}_{vi} - \boldsymbol{\vartheta}_{vj}|^2\right] \tag{24}$$

with

$$\begin{aligned}\mathcal{E}_{vi} :=& \frac{1}{2}\Big[m_iv_i^2 + |\dot{\boldsymbol{\vartheta}}_{vi}|^2\\ &+ 2k_{vi}\big[\ln(\cosh(\vartheta_{xi} - \bar{x}_i)) + \ln(\cosh(\vartheta_{yi} - \bar{y}_i))\big]\Big],\end{aligned}$$

$$\Upsilon_{vi} := \frac{1}{2\beta_i}\sum_{j\in\mathcal{N}_i}a_{ij}\bar{T}_{ji}\int_{-\bar{T}_{ji}}^0\int_{t+\eta}^t|\dot{\boldsymbol{\vartheta}}_{vj}(\sigma)|^2d\sigma d\eta, \quad \beta_i > 0.$$

The functional V is positive definite and radially unbounded, since so is $\ln(\cosh(\cdot))$ and $\Upsilon_{vi}(t)$ for all $t \geq 0$. Evaluating the total derivative along the trajectories of (20) we obtain

$$\begin{aligned}\dot{V} = -\sum_{i=1}^N\Bigg[&\frac{f_{vi}}{p_{vi}}v_i^2 + \frac{d_{vi}}{p_{vi}}|\dot{\boldsymbol{\vartheta}}_{vi}|^2 + \sum_{j\in\mathcal{N}_i}a_{ij}\dot{\boldsymbol{\vartheta}}_{vj}^\top\int_{t-\bar{T}_{ji}}^t\dot{\boldsymbol{\vartheta}}_{vj}(\sigma)\,d\sigma\\ &+\frac{1}{2\beta_i}\sum_{j\in\mathcal{N}}a_{ij}\bar{T}_{ji}\left(\int_{t-\bar{T}_{ji}}^t|\dot{\boldsymbol{\vartheta}}_{vj}(\sigma)|d\sigma - \bar{T}_{ji}|\dot{\boldsymbol{\vartheta}}_{vj}(t)|^2\right)\Bigg]\end{aligned}$$

which, after a successive application of Young and Cauchy-Schwartz inequalities leads to

$$\dot{V} \leq -\sum_{i=1}^N\left(\frac{f_{vi}}{p_{vi}}v_i^2 + \left[\frac{d_{vi}}{p_{vi}} - \sum_{j\in\mathcal{N}_i}a_{ij}\left(\frac{\beta_i}{2} + \frac{\bar{T}_{ji}^2}{2\beta_j}\right)\right]|\dot{\boldsymbol{\vartheta}}_{vi}|^2\right)$$

Hence, after (22), for each $i \leq N$, there exist constants c_{1i} and $c_{2i} > 0$ such that

$$\dot{V} \leq -\sum_{i=1}^N c_{1i}v_i^2 - c_{2i}|\dot{\boldsymbol{\vartheta}}_{vi}|^2 \leq 0. \tag{25}$$

From the above and the positivity of V it also follows that V is uniformly bounded and so are the trajectories. More precisely, v_i, $\boldsymbol{e}_{\vartheta_{vi}}$, $\dot{\boldsymbol{\vartheta}}_{vi}$, and $|\boldsymbol{\vartheta}_{vi} - \bar{\mathbf{z}}_i| \in \mathcal{L}_\infty$ for all $i \leq N$.

https://doi.org/10.58571/CNCA.AMCA.2024.059

Next, let us consider the angular-motion closed-loop equations $\Sigma_{\omega i}$ in (14) and the Lyapunov-Krasovskii functional

$$W := \sum_{i=1}^{N}\left[\frac{1}{p_{\omega i}}\mathcal{E}_{\omega i} + \Upsilon_{\omega i} + \frac{1}{4}\sum_{j\in\mathcal{N}_i} a_{ij}\left(\vartheta_{\omega i} - \vartheta_{\omega j}\right)^2\right]$$

where, for each $i \leq N$,

$$\mathcal{E}_{\omega i} := \frac{1}{2}\left[I_i\omega_i^2 + \dot{\vartheta}_{\omega i}^2 + 2k_{\omega i}\ln(\cosh\left(\vartheta_{\omega i} - \theta_i\right))\right],$$

$$\Upsilon_{\omega i} := \frac{1}{2\varepsilon_i}\sum_{j\in\mathcal{N}_i} a_{ij}\bar{T}_{ji}\int_{-\bar{T}_{ji}}^{0}\int_{t+\eta}^{t}|\dot{\vartheta}_{\omega j}(\sigma)|^2 d\sigma d\eta,$$

and $\varepsilon_i > 0$. The functional W is positive definite and radially unbounded in ω_i, $(\vartheta_{\omega i}-\theta_i)$, $\dot{\vartheta}_{\omega i}$, and $e_{\omega i}$. Also, its total time derivative along the trajectories of (14) using the Young and Cauchy Schwartz inequalities, yields:

$$\dot{W} \leq -\sum_{i=1}^{N}\left(\left[\frac{d_{\omega i}}{p_{\omega i}} - \sum_{j\in\mathcal{N}_i} a_{ij}\left(\frac{\varepsilon_i}{2} + \frac{\bar{T}_{ji}^2}{2\varepsilon_j}\right)\right]|\dot{\vartheta}_{\omega i}|^2 + \frac{f_{\omega i}}{p_{\omega i}}\omega_i^2 - \frac{1}{p_{\omega i}}\alpha_i\dot{\vartheta}_{\omega i}\right).$$

So, after (23), for each $i \leq N$, there exists $\lambda_{\omega i} > 0$ such that

$$\dot{W} \leq -\sum_{i=1}^{N}\left[\frac{f_{\omega i}}{p_{\omega i}}\omega_i^2 + \lambda_{\omega i}|\dot{\vartheta}_{\omega i}|^2 - \frac{1}{p_{\omega i}}\alpha_i\dot{\vartheta}_{\omega i}\right]. \quad (26)$$

Furthermore, note that α_i, which is defined in (15), is bounded; more precisely, $|\alpha_i| \leq \sqrt{2}\bar{\psi}_i k_{\alpha i}$. Hence, there exists $a > 0$ such that $\dot{W} \leq W + a$.

Following (Nuño et al., 2020, Proposition 1), the dynamics (12) is input-to-state-stable, with input $\nu_{\omega i}$ and state $\dot{\vartheta}_{\omega_i}, \tilde{e}_{\omega i}$. Since $\nu_{\omega i}$ is bounded, so are $\tilde{e}_{\omega i}$ and $\dot{\vartheta}_{\omega i}$. Then, after $\dot{\omega}_i$ in (14) we also conclude that $\omega_i \in \mathcal{L}_\infty$ and consequently $\dot{\omega}_i \in \mathcal{L}_\infty$.

By integrating along the trajectories on both sides of (25), and since V is also bounded, we have that v_i and $\dot{\boldsymbol{\vartheta}}_{vi} \in \mathcal{L}_2$. From the fact that $v_i \in \mathcal{L}_2 \cap \mathcal{L}_\infty$ and $\dot{v}_i \in \mathcal{L}_\infty$ it concludes by Barbălat's Lemma that $v_i \to 0$ as $t \to \infty$. Moreover, $\dot{v}_i$ is bounded from the fact that both terms on right-hand side of (20) are bounded. That $\dot{\boldsymbol{\vartheta}}_{vi} \to 0$ follows also from Barbălat's Lemma and the fact that $\dot{\boldsymbol{\vartheta}}_{vi} \in \mathcal{L}_2 \cap \mathcal{L}_\infty$ and $\ddot{\boldsymbol{\vartheta}}_{vi} \in \mathcal{L}_\infty$. The boundedness of $\ddot{\boldsymbol{\vartheta}}_{vi}$ follows by observing that all the terms on the right-hand side of (14) are bounded since

$$\boldsymbol{\vartheta}_{vi} - \boldsymbol{\vartheta}_{vj}(t - T_{ji}(t)) = \boldsymbol{\vartheta}_{vi} - \boldsymbol{\vartheta}_{vj} + \int_{t-T_{ji}(t)}^{t}\dot{\boldsymbol{\vartheta}}_{vj}(\sigma)d\sigma, \quad (27)$$

by adding all terms over $i \leq N$ on both sides of the equation, and in the view of (19), the expression can be defined in therms of $\boldsymbol{e}_{vi}$ such that $\boldsymbol{e}_{vi}$ and $\dot{\boldsymbol{\vartheta}}_{vj} \in \mathcal{L}_\infty$ for all $j \leq N$, and $|T_{ji}(t)| \leq \bar{T}_{ji}$ for all $t \geq 0$ and all $i, j \leq N$, it follows that $\tilde{\boldsymbol{e}}_{vi} \in \mathcal{L}_\infty$.

Next, convergence of $\dot{v}_i$ can be proven if $\dot{v}_i$ is uniformly continuous, which holds because all the terms on the right-hand side of

$$\ddot{v}_i = -\frac{1}{m_i}\Big(f_{vi}\dot{v}_i + k_{vi}\omega_i(t)\boldsymbol{\varphi}(\theta_i(t))^{\perp\top}\mathbf{tanh}(\bar{\mathbf{z}}_i - \boldsymbol{\vartheta}_{vi}) + k_{vi}\boldsymbol{\varphi}(t)(\theta_i(t))^\top\begin{bmatrix}\operatorname{sech}^2(\bar{x}_i - \vartheta_{xi})(\dot{\bar{x}}_i - \dot{\vartheta}_{xi})\\ \operatorname{sech}^2(\bar{y}_i - \vartheta_{yi})(\dot{\bar{y}}_i - \dot{\vartheta}_{yi})\end{bmatrix}\Big) \quad (28)$$

are bounded. Therefore, in view that

$$\lim_{t\to\infty}\int_0^t \dot{v}_i(\sigma)d\sigma = \lim_{t\to\infty} v_i(t) - v_i(0) = -v_i(0),$$

we conclude after Barbălat's Lemma that $\dot{v}_i \to 0$. Thus, from the latter, the fact that $v_i \to 0$, and $\dot{v}_i$ in (20), we obtain

$$\lim_{t\to\infty}\boldsymbol{\varphi}(\theta_i(t))^\top\tanh(\bar{\mathbf{z}}_i(t) - \boldsymbol{\vartheta}_{vi}(t)) = 0. \quad (29)$$

Similarly, it can be shown that $\ddot{v}_i \to 0$ since the last is uniformly continuous and the fact that $\dot{v}_i \to 0$. Which in turn, together with $\dot{\boldsymbol{\vartheta}}_{vi} \to 0$ and $\dot{v}_i \to 0$, imply from (28) that

$$\lim_{t\to\infty}\omega_i(t)\boldsymbol{\varphi}(\theta_i(t))^{\perp\top}\mathbf{tanh}(\bar{\mathbf{z}}_i(t) - \boldsymbol{\vartheta}_{vi}(t)) = 0. \quad (30)$$

After (29) and (30) we obtain that the trajectories converge to the manifold where both $\boldsymbol{\varphi}(\theta_i)^\top\tanh(\bar{\mathbf{z}}_i - \boldsymbol{\vartheta}_{vi}) = 0$ and $\omega_i\boldsymbol{\varphi}(\theta_i)^{\perp\top}\mathbf{tanh}(\bar{\mathbf{z}}_i - \boldsymbol{\vartheta}_{vi}) = 0$ hold. From this it can be established two cases in which this holds: either because $\lim_{t\to\infty}\boldsymbol{\varphi}(\theta_i(t))^{\perp\top}\mathbf{tanh}(\bar{\mathbf{z}}_i(t) - \boldsymbol{\vartheta}_{vi}(t)) = 0$, or because $\omega_i \to 0$.

In the first case, $\boldsymbol{\varphi}(\theta_i)^\perp$ and $\boldsymbol{\varphi}(\theta_i)$ belong to orthogonal spaces and (29) holds, necessarily, $\lim_{t\to\infty}\mathbf{tanh}(\bar{\mathbf{z}}_i(t) - \boldsymbol{\vartheta}_{vi}(t)) = \mathbf{0}$. Considering $\mathbf{tanh}(\bar{\mathbf{z}}_i - \boldsymbol{\vartheta}_{vi}) =: \nu_{vi}$ as an input, the equation $\ddot{\boldsymbol{\vartheta}}_{vi}$ resembles a network of Lagrangian systems as in (10). According to (Nuño et al., 2020, Proposition 1) these Lagrangian systems are input-to-state-stable and asymptotically stable when $\nu_{vi} \equiv 0$. Hence, since $\nu_{vi}(t) \to 0$ for all $i \leq N$, it follows that $\boldsymbol{e}_{vi} \to 0$. That is, $\lim_{t\to\infty}[\boldsymbol{\vartheta}_{vi}(t) - \boldsymbol{\vartheta}_{vj}(t)] = 0$, for all i, $j \leq N$, leading to the conclusion that

$$\lim_{t\to\infty}\bar{\mathbf{z}}_i(t) = \lim_{t\to\infty}\boldsymbol{\vartheta}_{vi}(t) = \mathbf{z}_c, \quad \forall\, i \leq N.$$

This means that consensus formation is achieved in the linear motion coordinates. Additionally, $\mathbf{tanh}(\bar{\mathbf{z}}_i(t) - \boldsymbol{\vartheta}_{vi}(t)) \to 0$ also implies that $\alpha_i \to 0$ along the systems' trajectories. Thus, the same vanishing-input argument as above leads to the conclusion that $\lim_{t\to\infty}\theta_i = \theta_c$, $\lim_{t\to\infty}\vartheta_{\omega i}(t) = \vartheta_c$, and $\lim_{t\to\infty}\omega_i(t) = 0$. This completes the proof for this scenario.

Alternatively, if (30) holds because $\omega_i \to 0$, differentiating both sides of $\dot{\omega}_i$; we obtain

$$\ddot{\omega}_i = -\frac{1}{I_i}\left[f_{\omega i}\dot{\omega}_i + k_{\omega i}\operatorname{sech}^2(\theta_i - \vartheta_{\omega i})(\omega_i - \dot{\vartheta}_{\omega i})\right]. \quad (31)$$

Then, since $\dot{\vartheta}_{\omega i}$ is bounded $\dot{\omega}_i \in \mathcal{L}_\infty$. We also conclude from (31) that $\ddot{\omega}_i \in \mathcal{L}_\infty$, implying that $\dot{\omega}_i$ is uniformly continuous. Similarly, following the same steps, it can be shown that $\omega_i^{(3)} \in \mathcal{L}_\infty$, making $\ddot{\omega}_i$ uniformly continuous

https://doi.org/10.58571/CNCA.AMCA.2024.059

as well. By applying Barbălat's Lemma successively, we conclude that $\dot{\omega}_i \to 0$ and consequently $\ddot{\omega}_i \to 0$.

Given the nature of tanh it follows from (14) that $|\theta_i - \vartheta_{\omega i}| \to 0$ and is bounded. Additionally, since $\operatorname{sech}^2(s)$ is bounded and separated from zero for all bounded $|s|$, we conclude from (31) that $\dot{\vartheta}_{\omega i} \to 0$.

The statement that $\ddot{\vartheta}_{\omega i} \to 0$ and $\vartheta^{(3)}_{\omega i} \to 0$ follows along similar lines as the proof of convergence for $\dot{\omega}_i$ and $\ddot{\omega}_i$ above, *i.e.*,. Given this, and the fact that v_i and $\dot{\boldsymbol{\vartheta}}_{vi} \to 0$, ensure that

$$\lim_{t\to\infty} \dot{\psi}_i(t)\boldsymbol{\varphi}(\theta_i)^{\perp\top}\mathbf{tanh}(\boldsymbol{\vartheta}_{vi}(t) - \bar{\mathbf{z}}_i(t)) = 0$$

and, since $\dot{\psi}_i(t)$ is persistently exciting (by assumption), it necessarily holds that

$$\lim_{t\to\infty} \boldsymbol{\varphi}(\theta_i)^{\perp\top}\mathbf{tanh}(\boldsymbol{\vartheta}_{vi}(t) - \bar{\mathbf{z}}_i(t)) = 0.$$

Again, in view of (29) and the orthogonality of $\boldsymbol{\varphi}(\theta_i)$ and $\boldsymbol{\varphi}(\theta_i)^{\perp}$, we have $\lim_{t\to\infty} \mathbf{tanh}(\bar{\mathbf{z}}_i(t) - \boldsymbol{\vartheta}_{vi}(t)) = 0$. The statement follows as in the previous case.

5. SIMULATIONS

In this section, we conduct simulations to validate our control scheme. We compare it with an unbounded variant, replacing $\tanh(s)$ with s. Five differential drive vehicles follow the communication topology depicted in Fig. 1 with interconnection weights set to one. Physical parameters and actuator bounds are outlined in Table 1, while initial conditions and offsets are provided in Table 2.

Table 1. Physical parameters and actuator bounds

Index	m_i [kg]	I_i [kg m^2]	R_i [m]	r_i [m]	$\bar{\tau}_i$ [N]
$1, 2$	1.52	0.4	0.12	0.0266	0.8
$3, 4$	1.9	0.5	0.15	0.0333	0.9
5	0.95	0.25	0.075	0.0166	0.7

Table 2. Initial conditions

Index	$x_i(0)$	$y_i(0)$	$\theta_i(0)$	δ_{xi}	δ_{yi}
1	4	10	$-3\pi/4$	0	5
2	10	10	$-\pi/2$	4.75	1.55
3	19	10	$3\pi/4$	2.95	-4.05
4	7	10	$\pi/2$	-2.95	-4.05
5	16	10	$-\pi/4$	-4.75	1.55

The control gains for each robot are determined to satisfy conditions (21), (22), and (23). These gains are defined as follows: $k_{vi} = 0.6$, $k_{\omega i} = 1$, $p_{vi} = 5.5$, $p_{\omega i} = 6$, $d_{vi} = 52$, $d_{\omega i} = 30$, and $k_{\alpha i} = 30$ for all $i \in N$.

The persistently exciting function $t \mapsto \psi_i(t)$ is defined as $\psi_i(t) := \frac{5}{4} + \sin(0.05t)$.

For a fair comparison, identical initial conditions, gains, and persistently exciting functions are used for both control schemes, constrained and unconstrained.

To simulate the time-delays in the system, we impose a uniform delay signal for all agents, emulating ordinary UDP/IP internet delays with a normal Gaussian distribution. The upper bound of these delays is set as $\bar{T}_{ji} = 0.65$s intentionally larger compared to real Internet delays.

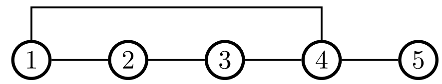

Fig. 1. Undirected-graph topology used in the numerical simulations

The vehicle paths in Figs. 2–3 show that both control schemes achieve the formation goal, with final orientations indicated by arrows. However, the unbounded scheme takes longer (Fig. 4) due to higher energy induced by unbounded actuators and the δ-persistently exciting function. Fig. 5 confirms this, showing that the unbounded scheme exceeds actuator bounds, while the proposed scheme stays within them.

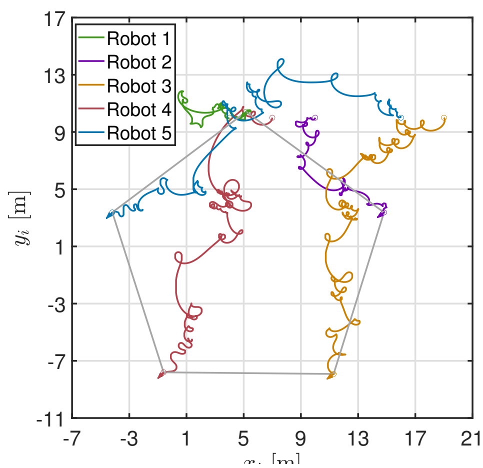

Fig. 2. Agent paths with the unbounded scheme.

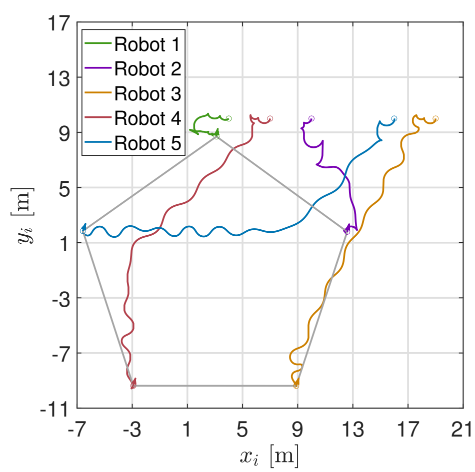

Fig. 3. Agent paths with the bounded scheme.

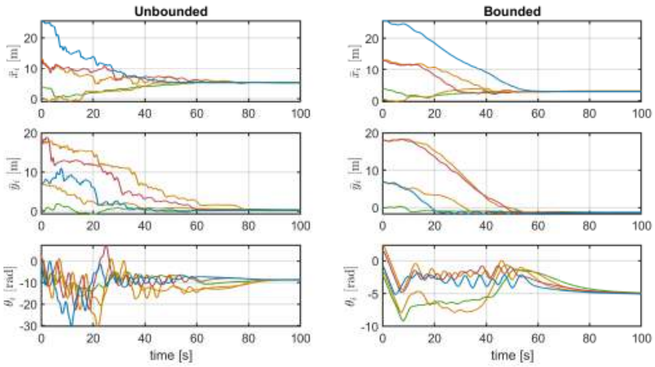

Fig. 4. Pose consensus comparison for both schemes.

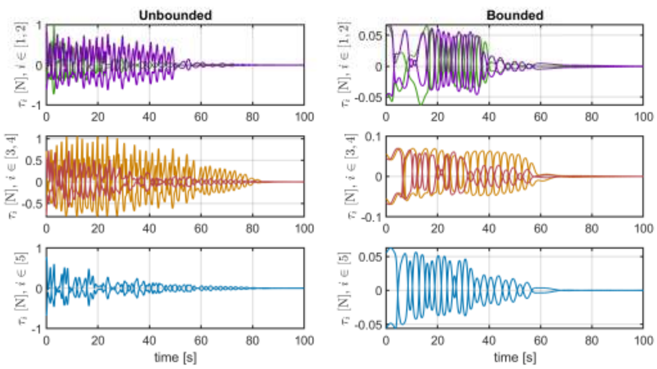

Fig. 5. Comparison of torque results for both schemes.

6. CONCLUSIONS

In this work we solve the consensus-based formation problem for multi-agent nonholonomic, considering realistic scenarios with variable-time delays and actuator saturation. Our proposed controller is dynamic, smooth, and adaptive, eliminating the need for velocity measurements by injecting damping through its second-order dynamics.

We assume a static, undirected interconnection topology among vehicles, but future work could explore dynamic or directed interconnections. Another avenue for future research is removing the assumption of differentiable time-delays.

REFERENCES

Ajorlou, A., Asadi, M., Aghdam, M., and Blouin, S. (2015). Distributed consensus control of unicycle agents in the presence of external disturbances. *Systems & Control Letters*, 82, 86–90.

Cao, Y. and Ren, W. (2011). *Distributed Coordination of Multi-agent Networks: Emergent Problems, Models, and Issues*. Springer-Verlag.

Cheng, Y., Jia, R., Du, H., Wen, G., and Zhu, W. (2018). Robust finite-time consensus formation control for multiple nonholonomic wheeled mobile robots via output feedback. *Int. J. Robust Nonlinear Control*, 28(6), 2082–2096.

Dimarogonas, D. and Kyriakopoulos, K. (2007). On the rendezvous problem for multiple nonholonomic agents. *IEEE Trans. Autom. Control*, 52(5), 916–922.

Hatanaka, T., Chopra, N., Fujita, M., and Spong, M. (2015). *Passivity-Based Control and Estimation in Networked Robotics*. Communications and Control Engineering. Springer.

Liang, X., Wang, H., Liu, Y., Chen, W., and Liu, T. (2018). Formation control of nonholonomic mobile robots without position and velocity measurements. *IEEE Trans. on Robotics*, 34(2), 434–446.

Lin, Z., Francis, B., and Maggiore, M. (2005). Necessary and sufficient graphical conditions for formation control of unicycles. *IEEE Trans. Autom. Control*, 50(1), 121–127.

Loría, A., Kelly, R., Ortega;, R., and Santibanez, V. (1997). On global output feedback regulation of euler-lagrange systems with bounded inputs. *IEEE Transactions on Automatic Control*, 42(8), 1138–1143.

Loría, A., Nuño, E., and Panteley, E. (2022). Observerless output-feedback consensus-based formation control of 2nd-order nonholonomic systems. *IEEE Trans. Autom. Control*, 67(12), 6934–6939.

Loría, A., Panteley, E., Popović, D., and Teel, A. (2005). A nested Matrosov theorem and persistency of excitation for uniform convergence in stable non-autonomous systems. *IEEE Trans. on Automat. Contr.*, 50(2), 183–198.

Nuño, E., Loría, A., and Panteley, E. (2022). Leaderless consensus formation control of cooperative multi-agent vehicles without velocity measurements. *IEEE Control Systems Letters*, 6, 902–907.

Nuño, E., Sarras, I., anbd M. Maghenem, A.L., Cruz-Zavala, E., and Panteley, E. (2020). Strict lyapunov-krasovskiĭ functionals for undirected networks of Euler-Lagrange systems with time-varying delays. *Systems and Control Letters*, 135, 104579.

Paredes-Lopez, A.I., Nuño, E., Cruz-Zavala, E., and Aldana, C.I. (2022). Output-feedback consensus of delayed networks of euler-lagrange agents with bounded controllers. *IEEE L-CSS*, 6, 1903–1908.

Peng, Z., Wen, G., Rahmani, A., and Yu, Y. (2015). Distributed consensus-based formation control for multiple nonholonomic mobile robots with a specified reference trajectory. *International Journal of Systems Science*, 46(8), 1447–1457.

Romero, J., Nuño, E., Restrepo, E., and Sarras, I. (2024). Global consensus-based formation control of nonholonomic mobile robots with time-varying delays and without velocity measurements. *IEEE Transactions on Automatic Control*, 69(1), 355–362.

Wang, H. (2014). Consensus of networked mechanical systems with communication delays: A unified framework. *IEEE Transactions on Automatic Control*, 59(6), 1571–1576.

Zavala-Río, A., Aguiñaga-Ruiz, E., and Santibáñez, V. (2011). Global trajectory tracking through output feedback for robot manipulators with bounded inputs. *Asian Journal of Control*, 13(3), 430–438.